JLab Program Advisory Committee Eleven Proposal Cover Sheet

This document must be received by close of business on Wednesday, December 18, 1996 at:

Jefferson Lab
User Liaison Office, Mail Stop 12 B
12000 Jefferson Avenue
Newport News, VA 23606

(Choose one)

☑ **New Proposal Title:** "Precision Measurement of the Nucleon Spin Structure Functions in the Region of the Nucleon Resonances"

☐ **Update Experiment Number:**

☐ **Letter-of-Intent Title:**

Contact Person

Name: Oscar A Rondon
Institution: Institute of Nuclear and Particle Physics, Univ of Virginia
Address: Physics Department
Address: McCormick Road
City, State ZIP/Country: Charlottesville, VA 22901
Phone: (804) 924-6787 **FAX:** (804) 924-4576
E-Mail › Internet: on@virginia.Edu

Experimental Hall: C **Days Requested for Approval:** 21

Jefferson Lab Use Only

Receipt Date: 17 DEC 96 PR-96-002

By: L Smith

BEAM REQUIREMENTS LIST

,Lab Proposal No.: _____ Date: _____

Hall: C Anticipated Run Date: _____ PAC Approved Days: _____

Spokesperson: Oscar A. Rondon Hall Liaison: R. Ciofini
Phone: (804) 924-6787
E-mail: OR@VIRGINIA.EDU

List all combinations of anticipated targets and beam conditions required to execute the experiment. (This list will form the primary basis for the Radiation Safety Assesment Document (RSAD) calculations that must be performed for each experiment.)

Condition No.	Beam Energy (MeV)	Mean Beam Current (μA)	Polarization and Other Special Requirements (e.g., time structure)	Target Material (use multiple rows for complex targets — e.g., w/windows)	Material Thickness (mg/cm²)	Est. Beam-On Time for Cond. No. (hours)
1	6000	≥ 0.06	≥ 80% longitudinal	NH_3	1476	220
		0.1 max	polarization	^4He	54	
				NMR coils (Cu)	85	
				Windows (Al)	117	
				Windows (Ti)	32	
				Total NH_3	1710	
2	6000	≥ 0.06	"	ND_3	1951	140
		0.1 max		^4He	54	
				NMR Coils	85	
				Windows (Al)	117	
				Windows (Ti)	32	
				Total ND_3	2239	

The beam energies, E_{Beam}, available are: $E_{Beam} = N \times E_{Linac}$ where N = 1, 2, 3, 4, or 5. E_{Linac} = 800 MeV, i.e., available E_{Beam} are 800, 1600, 2400, 3200, and 4000 MeV. Other energies should be arranged with the Hall Leader before listing.

HAZARD IDENTIFICATION CHECKLIST

JLab Proposal No.: _____ Date: _____
(For CEBAF User Liaison Office use only)

Check all items for which there is an anticipated need.

Cryogenics
- _____ beamline magnets
- _____ analysis magnets
- V target
  - type: Polarized
  - flow rate: 2-3 lit/h LH2
  - capacity: 60 Liter

Electrical Equipment
- _____ cryo/electrical devices
- _____ capacitor banks
- _____ high voltage
- _____ exposed equipment

Radioactive/Hazardous Materials
List any radioactive or hazadorous/ toxic materials planned for use:
Target: NH3, ND3 (~20 g each)

Pressure Vessels
- _____ inside diameter
- _____ operating pressure
- _____ window material
- _____ window thickness

Flammable Gas or Liquids
- type: _____
- flow rate: _____
- capacity: _____

Drift Chambers
- type: _____
- flow rate: _____
- capacity: _____

Other Target Materials
- ___ Beryllium (Be)
- ___ Lithium (Li)
- ___ Mercury (Hg)
- ___ Lead (Pb)
- ___ Tungsten (W)
- ___ Uranium (U)
- ___ Other (list below)

Vacuum Vessels
- _____ inside diameter
- _____ operating pressure
- _____ window material
- _____ window thickness

Radioactive Sources
- _____ permanent installation
- _____ temporary use
- type: _____
- strength: _____

Large Mech. Structure/System
- _____ lifting devices
- _____ motion controllers
- _____ scaffolding or
- _____ elevated platforms

Lasers
- type: _____
- wattage: _____
- class: _____

Installation:
- _____ permanent
- _____ temporary

Use:
- _____ calibration
- _____ alignment

Hazardous Materials
- ___ cyanide plating materials
- ___ scintillation oil (from)
- ___ PCBs
- ___ methane
- ___ TMAE
- ___ TEA
- ___ photographic developers
- V other (list below)

Ammonia (about 20 g in target ~100 g total)

General:

Experiment Class:
- _____ Base Equipment
- _____ Temp. Mod. to Base Equip.
- _____ Permanent Mod. to Base Equipment
- _____ Major New Apparatus

Other: _____

LAB RESOURCES REQUIREMENTS LIST

JLab Proposal No.: _____ Date: _____
(For CEBAF User Liaison Office use only.)

List below significant resources — both equipment and human — that you are requesting *from JLab* in support of mounting and executing the proposed experiment. Do not include items that will be routinely supplied to all running experiments, such as the base equipment for the hall and technical support for routine operation, installation, and maintenance.

***Major Installations** (either your equip. or new equip. requested from JLab)*

_____

_____

_____

_____

_____

_____

_____

_____

_____

New Support Structures: _____

_____

_____

Data Acquisition/Reduction

Computing Resources: _____

_____

_____

New Software: _____

_____

_____

Major Equipment

Magnets _____

_____

Power Supplies _____

_____

Targets _____

_____

Detectors _____

_____

Electronics _____

_____

Computer Hardware _____

_____

Other _____

_____

Other

_____

_____

_____

_____

_____

TJNAF PROPOSAL

Precision measurement of the nucleon spin structure functions in the region of the nucleon resonances

S. Bültmann, D.G. Crabb, C. Cothran, D. Day, E. Frlez,

J. S. McCarthy, P. McKee, D. Počanić, C. Smith,

O. Rondon-Aramayo (spokesman), A. Tobias and B. Zihlman

Institute of Nuclear and Particle Physics

Department of Physics, University of Virginia

Charlottesville, VA 22901, USA

J. Jourdan, T. Petitjean, I. Sick, G. Warren and J. Zhao

Department of Physics and Astronomy, Universität Basel, CH-4056, Basel, Schweiz

R. Carlini, J-P. Chen, J. Gomez, D. Mack,

J. Mitchell

Thomas Jefferson National Accelerator Facility

Newport News, VA, 23606

Abstract

We propose to make high precision and high resolution measurements of the spin structure of the proton and deuteron in the region of the nucleon resonances, at two values of Q^2: ~ 1 GeV^2 and ~ 5.5 GeV^2. Fundamental properties of the nucleon and QCD will be explored with adequate precision to obtain conclusive information. We plan to use TJNAF's polarized electron beam at 6 GeV, the Virginia-Basel solid polarized target with NH_3 and ND_3 materials and the Hall C High Momentum Spectrometer.

1. Motivation

The availability of polarized electron beams of 6 GeV or higher energies at TJNAF, substantially broadens the opportunities of physics experiments with polarized beams and targets. In particular, it opens up the feasibility of extending the studies of the nucleon spin structure beyond the D.I.S. region that is under current scrutiny in experiments at SLAC [1,2], CERN [3] and HERA [4], into the little known nucleon resonances region, for which only low resolution data are currently available [5,6]. The extensive past studies of the DIS nucleon spin structure functions at SLAC [7–13] and CERN [14,15], have established that the fraction of the proton spin carried by the quarks is 30%±5%. Our understanding of the nucleon spin for final state invariant mass $W < 2$ GeV is far less clear. New results from the low energy (9.7 GeV) data of SLAC Experiment 143 represent a valuable but limited improvement on our existing knowledge, due to lack of spectrometer resolution.

The objective of the experiment described in this proposal is to measure in detail the spin asymmetries for both the proton and the deuteron in the region of the nucleon resonances at two values of Q^2, combining the proven solid polarized target technology used at SLAC in E143, with the advantages offered by TJNAF's Hall C High Momentum Spectrometer (HMS), and the beam's unity duty factor, using essentially the same setup as that of Hall C experiments 93-026 [16] and 93-028 [17]. These advantages are:

- A large solid angle, 10 msr.
- More than adequate momentum resolution for the HMS ($dp/p = 0.3\%$)
- No count rate limitations due to high instantaneous current. A 100 nA average current, which is the highest that the polarized target has been shown to tolerate and still operate reliably is readily available.

With the momentum bite of the HMS (±10%) the region of interest can be covered with at most two settings, at any angle.

FIGURES

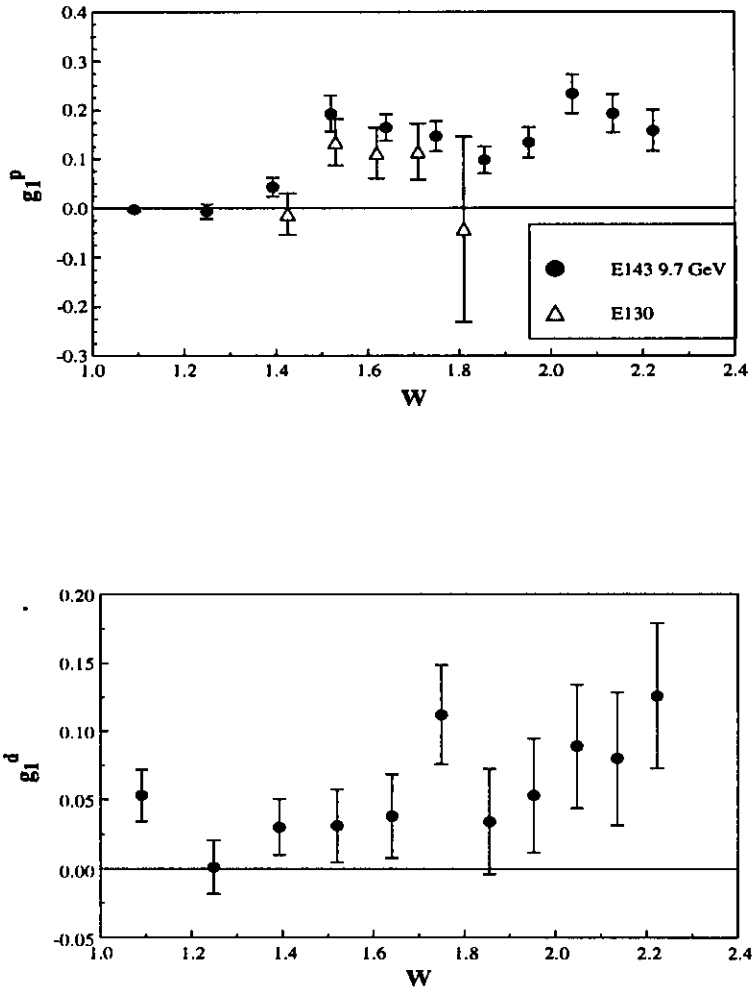

FIG. 1. The proton and deuteron spin structure functions in the nucleon resonances region. E143 results at 7° electron scattering angle (black circles) and E130 data (open triangles, converted to g_1^p from $A_1 + \eta A_2$, assuming $A_2 = 0$).

The available spin asymmetry data on the resonances region are limited to the old SLAC E130 [5] results with large uncertainties, and the recent data from SLAC E143 [6], which have marginal resolution. The situation is illustrated graphically in Fig.1. In spite of E143's good statistical uncertainties, the W range from the pion production threshold to the upper mass end of the first resonance could not be resolved in that experiment in better than three

bins. Both experiments measured only the asymmetry for longitudinally polarized electrons scattering on targets polarized parallel or antiparallel to the beam helicity. For this reason the interesting spin asymmetries A_1 and A_2 which at low energy have comparable kinematic coefficients, (see eq.(10)) could not be separated.

On the other hand, an experiment using TJNAF's Hall C HMS could measure the spin asymmetries accurately and with very good resolution in about three weeks running time, for both protons and deuterons. The Virginia-Basel polarized target used in E143 is capable of polarizing both protons and deuterons, and its magnetic field can be oriented in a broad range of angles relative to the lepton helicity or to the the three-momentum transfer $\mathbf{q}$, to study longitudinal and transverse asymmetries. This capability is fundamental for the separation of the A_1 and A_2 components

The nucleon spin structure functions $g_1(x)$ and $g_2(x)$, are fundamental quantities. In the limit of large momentum transfer g_1 and g_2 depend only on the Bjorken scaling variable x. g_1 is related to the longitudinal spin distribution. In the naive parton model (in the infinite momentum frame) all spins in the nucleon are aligned along the momentum axis. Polarized electrons scattering off longitudinally polarized nucleons should reflect the effects of the parton polarization. Specifically, the quark total helicity and helicity distributions are contained in g_1, and can be extracted with the aid of additional information. The Bjorken sum rule [18] relates the difference of the first moments of g_1^p and g_1^n (extracted from g_1^d) to the axial charge of the nucleon, using isospin symmetry. The deuteron integral can be expressed in terms of singlet and octet axial vector current matrix elements to obtain, with reasonable assumptions about $SU(3)_{flavor}$ symmetry, the most precise measurement of the quarks' contribution to the nucleon helicity (singlet matrix element).

The preceding picture is valid in the deep inelastic scattering regime, where the parton model works best. The related spin asymmetries $A_1(x, Q^2)$ and $A_2(x, Q^2)$ extend the meaning of the spin structure functions to the nucleon resonances region, which corresponds to x near 1, for $Q^2 \simeq 4$ GeV^2. At high x, QCD predicts that A_1 approaches 1: the leading quark carries all the spin. A_1 has only been measured up to $x = 0.8$ at $Q^2 \simeq 10$ GeV^2,with substan-

tial uncertainties due to low counting rates. In the absence of high x data the computation of the moments of the spin structure functions to test sum rules such as Bjorken's relies on extrapolations above $x = 0.8$ to $x = 1$ based on quark counting rules [19]. Measuring the asymmetries in the resonances region would test if such extrapolations for the asymmetries agree with the local (Bloom-Gilman [20]) duality observed for the unpolarized cross sections as it can be seen in fig. 2. Since the range $0.8 < x < 1$ corresponds to the resonances region for Q^2 up to 12 GeV^2, TJNAF's unity duty factor and good resolution are invaluable in dealing with the small and feature-rich cross sections observed in this kinematic region.

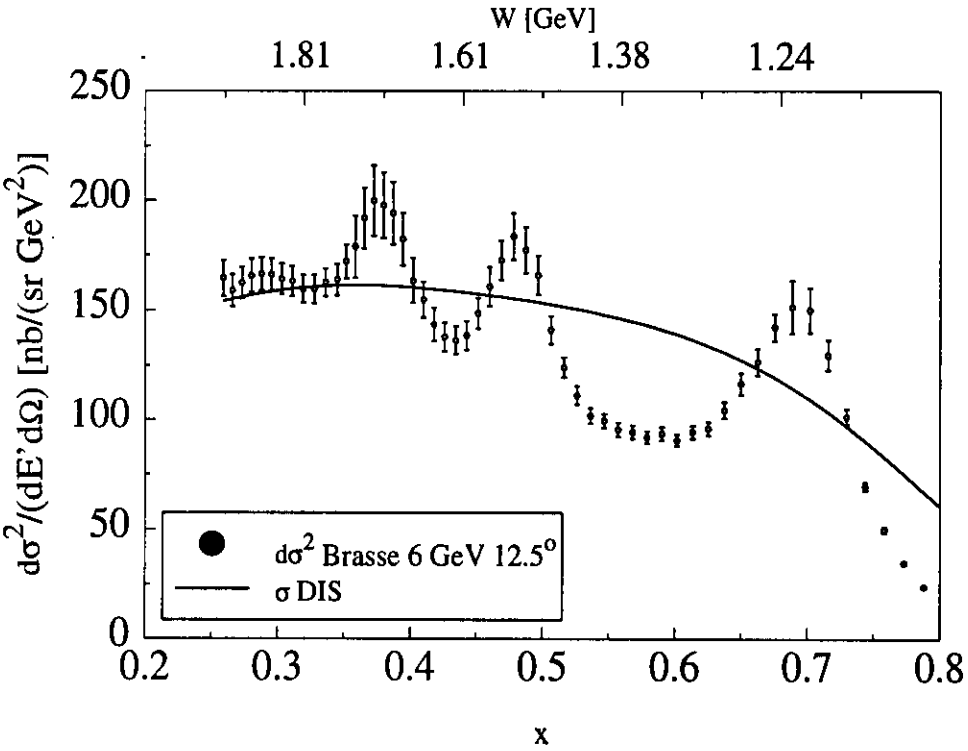

FIG. 2. The $e-p$ double differential cross section in the nucleon resonances region, at TJNAF kinematics. Also shown is the extrapolated DIS cross section.

In the naive parton model there is no room for transverse spin. However, in the operator-product expansion, transverse spin is included in the chiral-odd leading-twist transversity spin structure function. While this contribution is dominant in polarized parton-parton scattering, it is suppressed in electron DIS. Transverse spin effects in DIS receive significant contribution from twist-3 matrix elements that describe quark-gluon interactions [21,22].The

spin asymmetry $A_2(x,Q^2)$, related to $g_2(x)$, receives its dominant contribution from the transverse asymmetry. Since higher twist effects have a $1/Q^{twist-2}$ evolution, TJNAF is a unique facility to study the low Q^2 properties of this fundamental asymmetry.

The improvements in our understanding of the spin structure of the nucleon resonances that would result from this experiment, will encompass a broad range of areas of fundamental nuclear physics. These range from a definitive determination of the sign of the asymmetry in the region of the $\Delta(1232)$ resonance, for which there is only a single data point with large errors at $x = 0.45$ and $Q^2 = 0.5$ GeV^2 [5], to precise information on both the longitudinal and transverse asymmetries in the region of the elusive Roper resonance, and valuable complementary data on the asymmetries in a region of Q^2 where the extended Gerasimov-Drell-Hearn [25] sum rule

$$I(Q^2) = \int_{Q^2/2m\nu}^{\infty} g_1^p(\nu,Q^2)\frac{d\nu}{\nu} = \frac{2m^2}{Q^2}\int_0^1 g_1^p(x,Q^2)dx = \Gamma(Q^2) \qquad (1)$$

is expected to have a change of sign.

The data at high Q^2 would constitute an unambiguous test of the pQCD prediction [29] that the electric quadrupole transition amplitude E_2 for the Δ resonance becomes comparable to the magnetic dipole M_1 in that kinematic regime. The determination of the asymmetry in the higher mass resonances region would provide an indispensable connection to the deep inelastic scattering region that is being intensively studied at the same kinematics in the current nucleon spin structure experiments, in particular the second generation ones. [1,2].

These results also would find application in more technical but still very important areas such as the radiative corrections for polarized electrons scattering on polarized targets, for which the main source of error comes from the lack of data in the resonance region. In summary, this experiment would yield major physics results for a minimal investment in beam time.

2. Polarized lepton scattering formalism

When longitudinally polarized leptons are incident on polarized nuclei one can compute

the sum and the difference of the cross sections for two opposing orientations θ_N and $\theta_N + \pi$ of the nucleon spin. The sum is just twice the unpolarized cross section, while the difference [30], [31] is sensitive to the nucleon polarization. For $\theta_N = 0$ (i.e. longitudinally polarized leptons and nucleons) we get

$$\frac{d^2\sigma(0)}{d\Omega dE'} - \frac{d^2\sigma(\pi)}{d\Omega dE'} = \sigma^{\uparrow\uparrow} - \sigma^{\uparrow\downarrow} = \frac{4\alpha^2 E'}{Q^4 E}((E + E'\cos\theta)MG_1(\nu, Q^2) - Q^2 G_2(\nu, Q^2)) \quad (2)$$

and for $\theta_N = \pi/2$ (longitudinal leptons and transverse nucleons) the result is

$$\frac{d^2\sigma(\pi/2)}{d\Omega dE'} - \frac{d^2\sigma(3\pi/2)}{d\Omega dE'} = \sigma^{\uparrow\rightarrow} - \sigma^{\uparrow\leftarrow} = \frac{4\alpha^2 E'}{Q^4 E} E' \sin\theta(MG_1(\nu, Q^2) + 2EG_2(\nu, Q^2)) \quad (3)$$

where θ is the lepton scattering angle, Ω is the lepton detector solid angle, M is the nucleon mass, and $\nu = E - E'$ is the energy transfer; E and E' are the beam and final electron energies.

$G_1(\nu, Q^2)$ and $G_2(\nu, Q^2)$ are the spin structure functions. They can be related in the asymptotic limit to helicity distributions of the partons in the nucleon:

$$\lim_{Q^2,\nu\to\infty} (M\nu)MG_1(\nu, Q^2) = g_1(x), \qquad \lim_{Q^2,\nu\to\infty} (M\nu)\nu G_2(\nu, Q^2) = g_2(x). \quad (4)$$

that are functions of the Bjorken scaling variable $x = Q^2/(2M\nu)$.

An equivalent approach can be followed starting from the virtual photon absorption cross sections for photon helicities +1, -1, 0: $\sigma^T_{1/2}, \sigma^T_{3/2}, \sigma^{TL}_{1/2}$, from which the spin asymmetries A_1, A_2 are constructed:

$$A_1 = \frac{\sigma^T_{1/2} - \sigma^T_{3/2}}{\sigma^T_{1/2} + \sigma^T_{3/2}} = \frac{M\nu G_1(\nu, Q^2) - Q^2 G_2(\nu, Q^2)}{W_1(\nu, Q^2)} \quad (5)$$

$$A_2 = \frac{\sigma^{TL}}{2\sigma^T} = \frac{\sqrt{Q^2}(MG_1(\nu, Q^2) + \nu G_2(\nu, Q^2))}{W_1(\nu, Q^2)} \quad (6)$$

where $2\sigma^T = \sigma^T_{3/2} + \sigma^T_{1/2}$. This approach involves the unpolarized structure function $W_1(\nu, Q^2) = (W^2 - M^2)\sigma^T/(8M\pi\alpha^2)$, which must be obtained from the more accessible ones $\nu W_2(\nu, Q^2) = F_2(\nu, Q^2)$ and $R(x, Q^2) = \sigma_L/\sigma_T$ using $W_1/W_2 = (1 + \nu^2 Q^2)/(1 + R)$.

The spin asymmetries are related to the measured asymmetries for the longitudinal and transversal configurations of the beam and target spins (known as $A_{||}$ and $A_{\perp}$, $A = (\sigma^{\uparrow\uparrow} - \sigma^{\uparrow\downarrow})/(\sigma^{\uparrow\uparrow} + \sigma^{\uparrow\downarrow})$) by expressions that involve kinematical factors, as well as the unpolarized structure function $R(x, Q^2)$.

$$A_1 = \frac{C}{D}\left(A_{||} - dA_{\perp}\right) \tag{7}$$

$$A_2 = \frac{C}{D}\left(c'A_{||} + d'A_{\perp}\right) \tag{8}$$

where $C = 1/(1 + \eta c')$, $\eta = \epsilon\sqrt{Q^2}/(E - \epsilon E')$, $c' = \eta(1 + \epsilon)/(2\epsilon)$, $\epsilon^{-1} = 1 + 2[1 + (\nu^2/Q^2)]\tan^2(\theta/2)$ is the usual longitudinal polarization of the virtual photon, $D = (1 - \epsilon E'/E/)/(1 + \epsilon R)$ is the virtual photon depolarization factor which is a function of R, $d' = 1/\sqrt{2\epsilon/(1 + \epsilon)}$ and $d = \eta d'$.

The connection between A_1 and the spin structure functions g_1 and g_2 is given by

$$\frac{g_1}{F_1} = A_1 + \frac{\gamma^2 g_2}{F_1} \tag{9}$$

where $\gamma = Q^2/\nu^2$ and $F_1 = MW_1$.

Experiments that measure only $A_{||}$ cannot separate A_1 and A_2, unless additional measurements with different beam energies at the same scattering angle are made, since both spin asymmetries are related to $A_{||}$ by

$$A_{||} = D(A_1 + \eta A_2). \tag{10}$$

The coefficient η ranges from ~ 1 at $W = 1.17$ GeV to ~ 0.35 at $W = 2$ GeV, so the contribution of A_2 cannot be neglected. The recent results from E143 [13] indicate that A_2 is $\sim 0.12A_1$ for $Q^2 = 3$ GeV^2, $0.53 < x < 0.75$ and shows no Q^2 dependence, within uncertainties. Although the E143 results apply to the deep inelastic region, we can use the average ratio A_2/A_1 at these high x values to estimate that the total A_2 contribution to $A_{||}$ may be $\geq 12\%$.

3. Test of perturbative QCD

A very interesting application of the asymmetries data to be measured at high Q^2 in this experiment is the testing of the pQCD prediction concerning helicity conservation in the N-Δ (1232) transition [29]. Past studies of the Q^2 dependence of the transition form factors for this and other resonances [32,33] are not conclusive, although there are indications that the form factors for the second and third resonance regions approach the pQCD behavior at $Q^2 > 3$ GeV^2, while the Δ shows a faster decrease than the Q^{-4} expected dependence.

Large statistical uncertainties due to low count rates at high Q^2 and contributions from non-resonant processes complicate the extraction of the form factors in inclusive experiments. An exclusive experiment to measure the form factors up to $Q^2 = 6$ GeV^2 has been approved for Hall B [34]. A similar experiment restricted to the Δ and $Q^2 = 4$ GeV^2 has also been approved and run in Hall C [35]. In both cases, unpolarized beam and targets are contemplated. In the present case, the use of polarization degrees of freedom provides a powerful handle to explore the properties of the the asymmetries at high momentum transfer.

As an illustration the asymmetry for photo- or electroproduction of the Δ is expected to approach -1 in the perturbative regime. This is due to the electric quadrupole form factor E_2 (or E_{1+}) becoming dominant: $E_2 = \sqrt{3}M_1$, because a double spin flip is involved in the process $N_{1/2} + \gamma_{-1} \rightarrow \Delta_{-3/2}$, where the subscripts refer to the helicities of the particles. This process is described by the helicity amplitude $G_- = \sqrt{4\pi}(-\sqrt{3}M_1 + E_2)/2$, which is strongly suppressed by helicity conservation. (The asymptotic relation between the multipoles is obtained by setting $G_- = 0$). A measurement of the related asymmetry $A_{TT} (\simeq A_1)$

$$A_{TT} = \frac{M_1^2 - E_2^2 - 6Re(E_2^* M_1/\sqrt{3})}{k_L C_2^2 + 2M_1^2 + 2E_2^2} = _{lim Q^2 \rightarrow \infty} -1 \qquad (11)$$

to a precision of $\sim$0.1 (absolute) would be a conclusive test ($\simeq$10% relative) if the asymmetry were of order unity and negative, and would establish a reasonable upper bound for the E_2/M_1 ratio at the proposed $Q^2 = 5.7$ GeV^2, if the perturbative regime turns out to set in at even higher momentum transfers. Such result would stand out in dramatic contrast with the extrapolation of the asymmetry from the DIS regime to the resonances region.

The extrapolation is shown in fig. 3, based on a world fit to $A_1(x, Q^2)$ [12] as a function of invariant mass W, for our proposed kinematics. The solid line is the world fit to g_1/F_1. The dashed line is A_1 obtained from g_1/F_1 (eq. 9) assuming that g_2 is only twist-2, an assumption entirely consistent with the E143 results [13] for g_2. The extension of local duality to polarized scattering would require that the resonance asymmetries average out to the DIS extrapolation: A large negative asymmetry at the first resonance, such as the one predicted by PQCD, would have to be compensated by at least as large positive asymmetries at the higher mass resonances.

In summary, these high Q^2 studies would yield high physics benefits for a minimal cost of beam time.

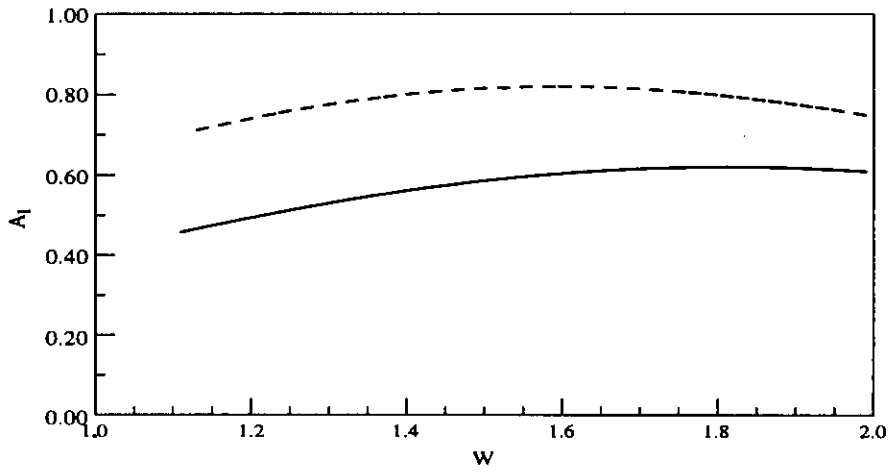

FIG. 3. World fit to g_1/F_1 for the proton (solid line) and resulting A_1 (dashed line) vs W.

4. Kinematic coverage

As we can see from Fig. 4, the nucleon resonances region covers a very large fraction of the x range for low beam energies, the kinematic region $0.2 \leq x \leq 1$ at $Q^2 \sim 1$ GeV^2 is accessible. This region would be accessible at TJNAF's beam energies (≤ 6 GeV) at a 12.5° angle. At greater scattering angles, even higher Q^2 values are reachable, and the resonances

move closer to $x = 1$, but the final energy interval

$$\frac{\Delta E'}{E'} = \frac{2(\,W_h{}^2 - \,W_l{}^2)}{2\,M^2 + 4\,EM - \,W_l{}^2 - \,W_h{}^2} \tag{12}$$

depends only on the invariant mass range $W_h - W_l$ and the beam energy E. For $E = 6$ GeV, $W_l = 0.938$ GeV ($= M$) and $W_h = 2$ GeV ($<Q^2>$ 1.3 Gev^2), $\Delta E'/E' = 0.32$, so two spectrometer settings are needed. For $E = 4$ GeV three settings are needed, making low Q^2 measurements less attractive, at any angle.

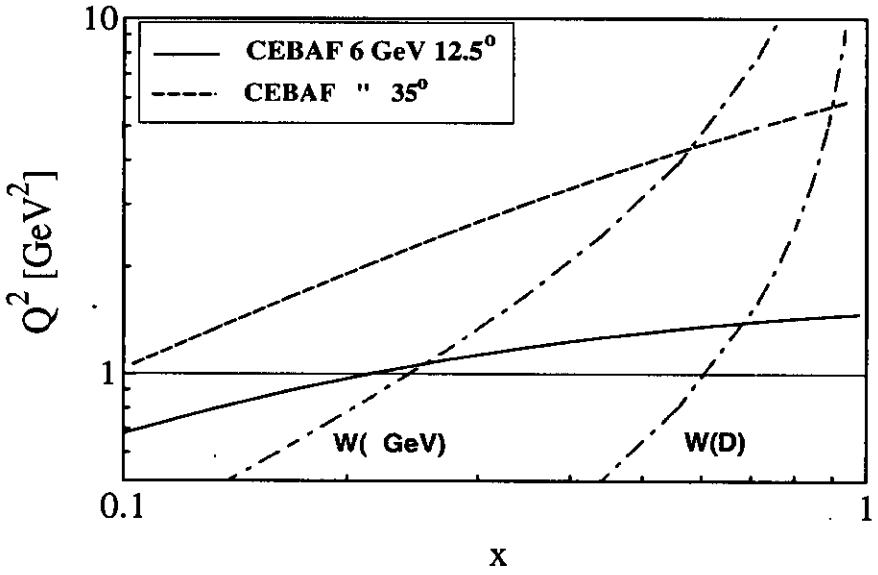

FIG. 4. The kinematic range accessible at 6 GeV beam energy and two angles. The dot-dashed curves are lines of constant W. The constant $Q^2 = 1$ GeV^2 is indicated.

At 35° the average Q^2 is 5.22 GeV^2, but it is 5.7 GeV^2 at the top of the $\Delta(1232)$. This is a sufficiently high value of Q^2 to test the pQCD prediction. The momentum bite and the upper and lower limits of the final electron energy are related by

$$E'_l = E'_h \frac{1 - \frac{\Delta p}{p}}{1 + \frac{\Delta p}{p}}. \tag{13}$$

For $E'_h = 4.984$ GeV, (corresponding to the π production threshold, W_l =1.17 GeV) a value

E'_l = 4.130 GeV, corresponding to W_h =1.83 GeV, is attainable in one momentum setting, so most of the three resonances region can be covered in a single run at 35°.

5. Experimental equipment.

The equipment needed to carry out the proposed experiment is summarized below:

• Polarized 6 GeV electron beam, $\geq$ 80% longitudinal polarization, 60 to 100 nA beam current.

• TJNAF's Hall C HMS spectrometer in a tune that combines a 10 msr solid angle, $\simeq$ 0.3% momentum resolution and $\pm$ 10% momentum bite.

• The normal HMS detector package to identify electrons and reject pions.

• The Hall C Møller polarimeter.

• The Virginia-Basel polarized target, with $\geq$ 85 % NH_3 polarization and $\geq$ 30% ND_3 polarization.

• Data acquisition system (electronics, hardware and software) capable of $\sim$ 1 kHz event rate.

All necessary equipment is available, no new hardware is required.

6. Count Rates and running times

The count rate of scattered electrons from the polarized target is given by

$$R = \frac{\mathcal{L}\mathcal{A}}{f}\frac{d\sigma^2}{d\Omega dE'} \tag{14}$$

where the luminosity $\mathcal{L} = 1 \times 10^{35}$ cm^{-2}Hz combines a 100 nA beam current with $\simeq 3 \times 10^{23}$ cm^{-2} thickness for the 3 cm long ^{15} NH_3 and ^{15} ND_3 solid polarized targets. The acceptance $\mathcal{A} = \Delta E' \Delta\Omega \simeq 0.4$ GeV msr corresponds to 30 MeV ΔW increments (which translate into $\Delta E' = 30$ MeV near the π threshold and $\Delta E' = 54$ MeV at $W = 1.95$ GeV) combined with the HMS solid angle $d\Omega = 10$ msr. The $e-p$ resonance scattering cross section $d\sigma^2/(d\Omega dE')$ is based on Brasse's [36] parameterization, and its corrected by the dilution factor f, which takes into account the fact that both polarized nucleons (3 H) and unpolarized nucleons (^{15}N, ^{4}He and other materials) are present in the target:

$$f = \frac{N_p\sigma_p}{N_p\sigma_p + N_{15N}\sigma_{15N} + N_{other}\sigma_{other}} \tag{15}$$

where $N_i = \rho_i m_i p_f$ is the number of nuclei of type i present in the target, ρ is the density of the material, m is the molecular weight, and p_f is the fraction of the target volume occupied by the material (packing fraction). The cross sections are per-nucleon $d\sigma^2(E,\theta)/(d\Omega dE')$ appropriate to the kinematic regime (resonances region). This implies that the neutron and proton cross sections are approximately the same, and that the dilution factor is close to $3/(3+15+\varepsilon)\approx 0.13$ where $\varepsilon \leq 5$ is the contribution of He and other materials.

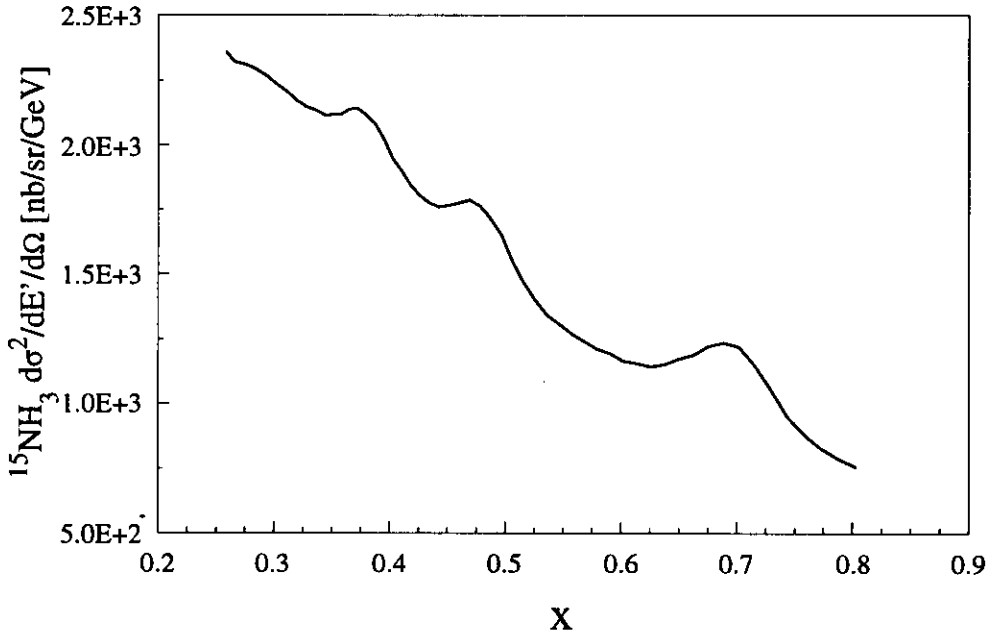

FIG. 5. Ammonia ($^{15}NH_3$) cross section from a combination of ^{15}N and 3 times the resonance $e-p$ cross section.

Of course, the presence of nitrogen and other materials in the target smears out the resonance shapes that stand out when the target is only hydrogen. Moreover, corrections must be applied to the measured asymmetries, to account for the small contribution of ^{15}N to the target polarization [10]. Fig. 5 shows a representative shape of the expected spectrum in the region of interest. The cross section for ammonia shown in this plot was constructed from a y-scaling model of ^{12}C [37] calculated for similar kinematic conditions ($E = 6$ GeV, $\theta = 13°$), and normalized to ^{15}N, plus three times the $e-p$ resonance cross section [36].

For deuterated ammonia $^{15}ND_3$ the definitions are similar, with the appropriate substi-

tutions of D for p. The numerical value can be approximated by $6/(6+15+5)\approx 0.23$.

Table 1 presents representative values of the rates for the proton for different values of W. The cross section is from ref. [36], combined with a quasielastic tail contribution [37] that extends down to $x \sim 0.5$. Also shown is the extrapolated DIS cross section (displayed in fig.2) from SLAC's L.W. Whitlow [39,38] global fits to the unpolarized structure functions F_2 and R, which are appropriate for our chosen kinematics. The rates are for $\Delta W = 15$ MeV intervals, and include electrons scattered from all the materials in the target. The total rate for the full spectrometer acceptance at the central momentum setting p_0'= 4.74 GeV/c (W = 1.49 GeV) is $\sim$ 1000 Hz.

Table 1. Kinematic variables, rates and cross sections.

W	x	Q^2	ϵ	E'	$d^2\sigma/dE'/d\Omega$	Rate	$d^2\sigma$ DIS
[GeV]		[GeV^2]		[GeV]	[nb/(sr GeV)]	[Hz]	[nb/(sr GeV)]
1.170	0.744	1.418	0.960	4.984	69.7	10.1	90.2
1.230	0.689	1.399	0.958	4.918	151.5	21.5	114.5
1.440	0.526	1.325	0.946	4.658	111.1	17.7	150.5
1.530	0.469	1.290	0.940	4.534	172.7	29.2	156.1
1.605	0.426	1.259	0.934	4.426	137.9	24.5	159.1
1.680	0.387	1.226	0.926	4.312	194.1	36.1	160.9
1.930	0.280	1.108	0.893	3.894	165.7	47.2	157.0

The number of counts needed for a given statistical uncertainty $\delta A_{||,\perp}$ in the measured asymmetries $A_{||}$ and $A_\perp$ is given by

$$N = \frac{1}{(f P_b P_t \delta A)^2}, \tag{16}$$

where P_b and P_t are the beam and target polarizations. Conversely, a data taking run of fixed duration $t = N/R$ determines the magnitude of δA. We have chosen the latter approach. For the main momentum setting ($W = M$ to 1.71 GeV) we fixed t = 40 hours of beam with P_b = 80%, on a $^{15}NH_3$ target with average longitudinal P_H = 85%, and t = 60 h on $^{15}ND_3$, with the same beam polarization, and P_D = 30%. A second momentum setting is needed

(1.47 GeV$\leq W \leq$ 2 GeV) to cover the full resonances' range. For this setting $t = 20$ hours for protons and $t = 30$ hours for deuterons is sufficient because the rates increase with W.

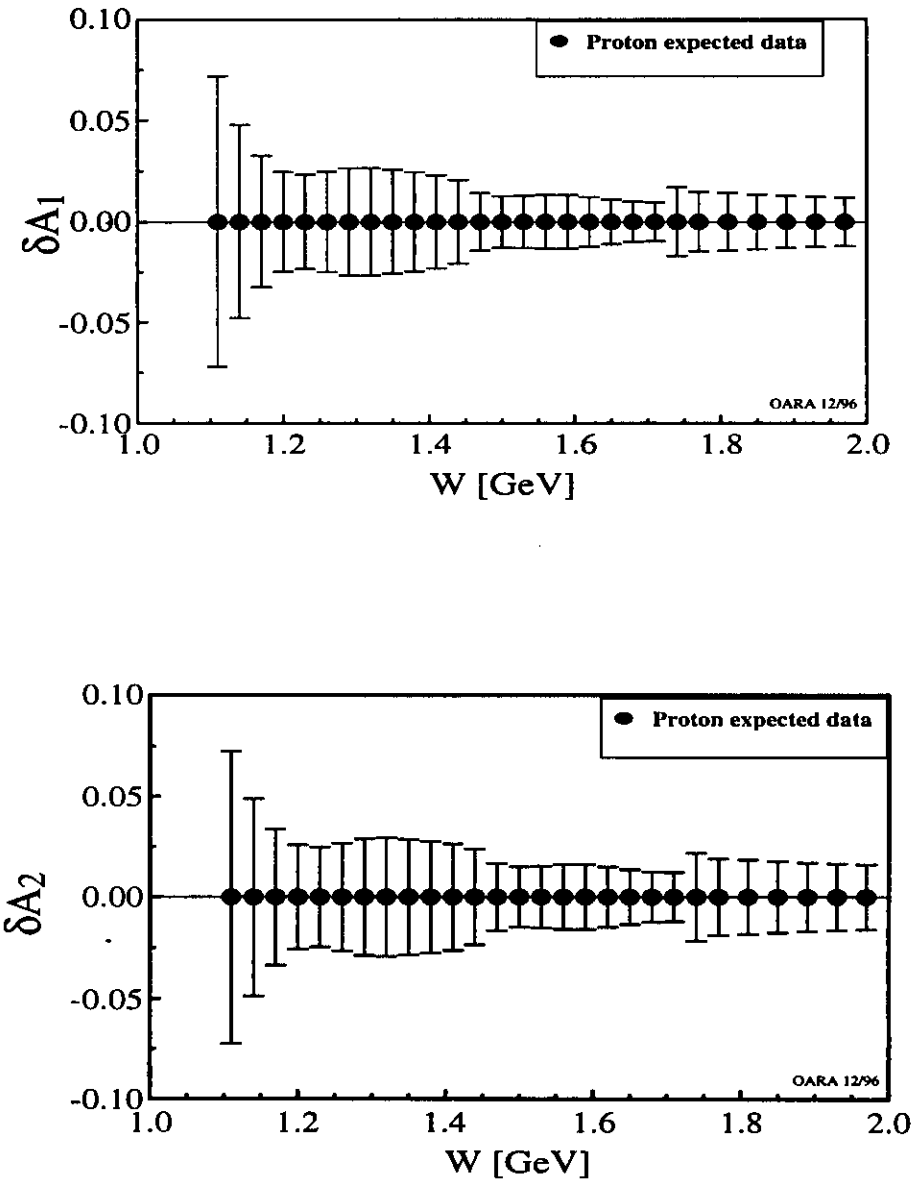

FIG. 6. Expected results for the proton plotted vs W for A_1(top) and A_2(bottom).

The expected results for the proton are shown in fig. 6. and those for the deuteron in fig. 7. We have computed the statistical uncertainties in A_1 and A_2 for both proton and

deuteron. We propagated the expected errors from $\delta A_{||}$ and $\delta A_{\perp}$ using the corresponding expressions for A_1 and A_2 in terms of the measured asymmetries, eqs. 7 and 8. The data will be binned in $\Delta W = 30$ MeV intervals. The uncertainties reflect the variation in counting rates for different invariant masses, and the improved statistics in the overlap region of the two central momentum settings.

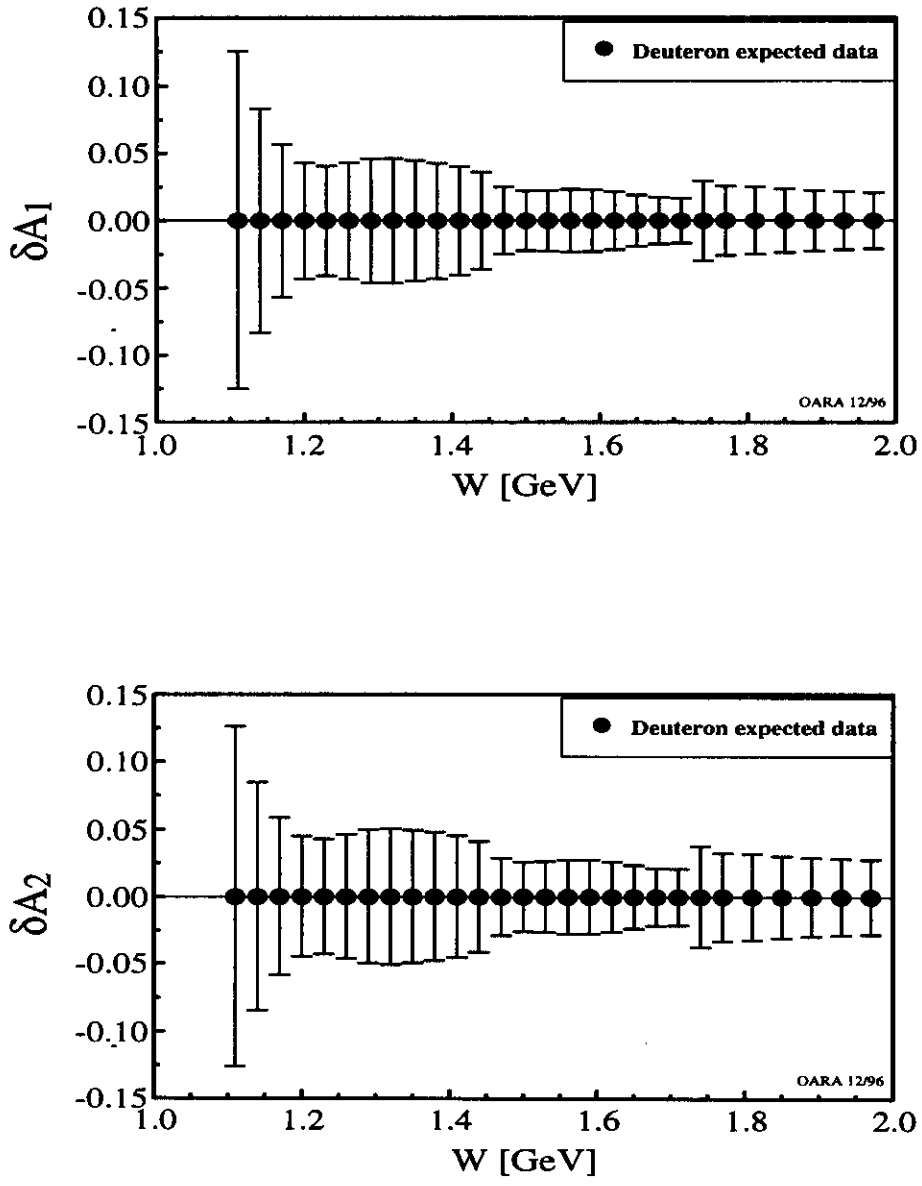

FIG. 7. Expected results for the deuteron plotted vs W for A_1(top) and A_2(bottom).

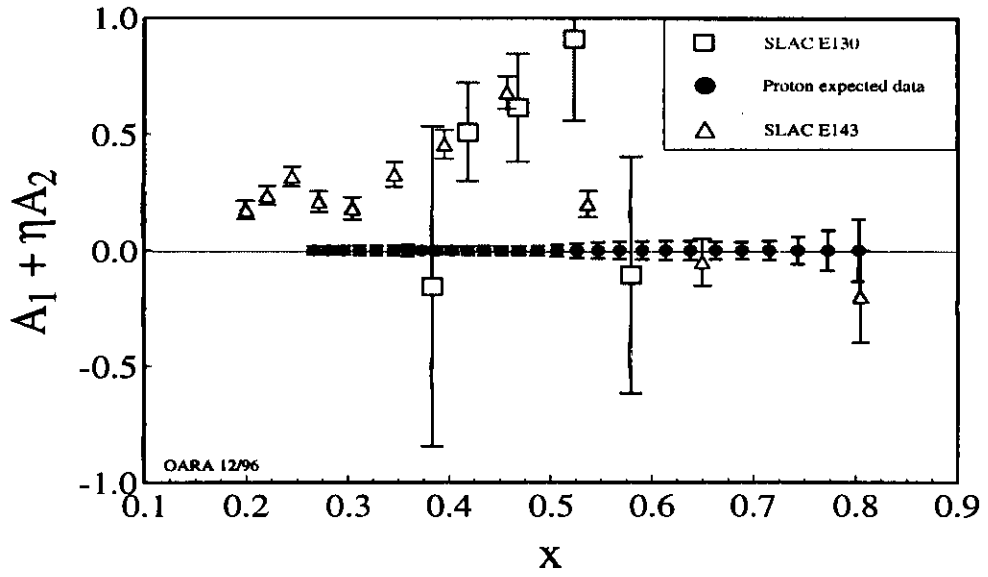

FIG. 8. The proton spin asymmetries $A_1 + \eta A_2$ in the nucleon resonances region, current data (E130, open squares, E143 open triangles) and expected errors (black circles).

The expected errors in terms of the combination $A_1 + \eta\ A_2$ are shown in fig. 8, along with the E130 results and the E143 g_1 data converted to $A_1 + \eta\ A_2$.

For the high Q^2 measurements, we assume the same values for the luminosity, spectrometer solid angle, and beam and target polarizations. $^{14}NH_3$ will be used as target (dilution factor $f \approx 0.16$) since the neutron polarization in ^{14}N is not a problem for this measurement, as it is for A_1^p. The invariant mass interval is again $\Delta W = 30$ MeV. For fixed data taking time $t \sim 150$ hours, the statistical error in the asymmetry A_{TT} is 0.15. The corresponding expected uncertainties are shown in fig. 9, for two possible values of the asymmetry, large (0.8) and 0.

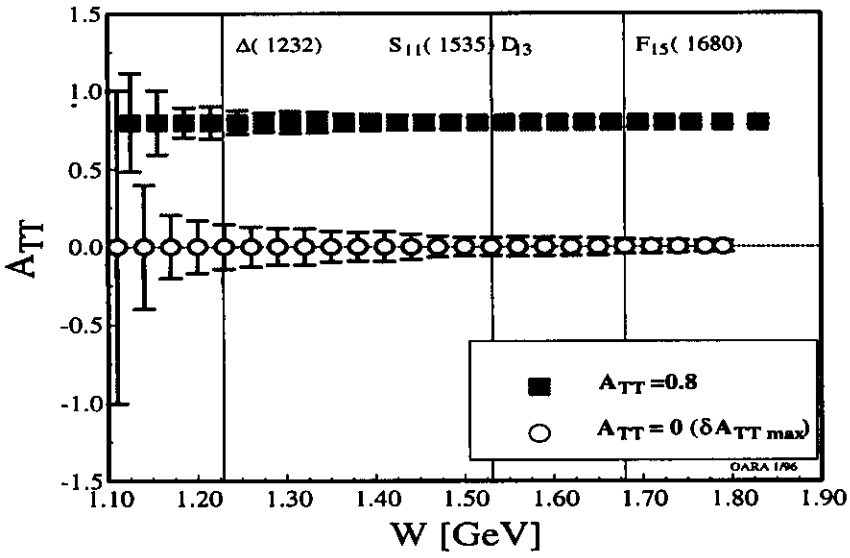

FIG. 9. Expected results for A_{TT} plotted vs W.

7. Transverse asymmetry.

The separation of the two asymmetries A_1 and A_2 requires a measurement of the transverse asymmetry $A_\perp$. This is a necessary condition to understand the spin asymmetries in more depth than just stating the positivity limit $|A_2| \leq R$, which seems to be marginally obeyed in DIS at high x [13]. Taking data in the transverse target field configuration for one half of the time devoted to the longitudinal configuration, will reduce the errors in A_1 due to $A_\perp$ to a negligible contribution (a 14% average increase in the statistical errors of A_1), and will increase our knowledge of A_2 infinitely. Taking data for a shorter time may not be efficient, considering the overhead involved.

Transverse runs during E143 did not present any unforeseen complications. A chicane, which will be used in experiment TJNAF 93-026, is required to compensate for the beam deflection due to the target field. The higher beam energy of this proposal compared to the ones planned for those Hall C experiments, simplifies somewhat the requirements, since smaller vertical deflections are involved, both for the incident as well as the scattered electrons. The rotation of the target from the longitudinal to the transverse field orientation

was done in E143 in less than one 8 hour shift, with the magnet at liquid He temperature.

For the measurement of A_{TT}, the target field has to be oriented along the three-momentum transfer **q** vector. At the chosen kinematics, this vector ranges from 15° at $W = 2$ GeV to 21.4° at the Δ. The optimum orientation will be chosen based on the constraints presented by the actual effective angular clearance of the target magnet in the forward direction (nominally $\pm$ 50° relative to the magnet axis).

8. Sources of Systematic Error

The systematic errors involved in spin asymmetry studies come mainly from the nature of the beam and target used. A growing number of experiments (SLAC E80, E130, E142, E143 and E154, CERN EMC and SMC, HERA HERMES) using polarization degrees of freedom have studied in great detail these and other sources of error. The table below gives conservative estimates of the most significant sources of error expected in the present proposal.

Essentially the same systematic errors are present for both the low and high Q^2 parts of the experiment.

Table 2. Sources of systematic error

Source	Proton	Deuteron
Beam P_b	2%	2%
Target P_t	2.5%	4%
Dilution f	2%	2%
Nitrogen correction	< 1%	1%
Pion contamination	< 1%	< 1%
Dead time	< 1%	< 1%
Radiative corrections	2%	6%
Errors from R and F_2	3%	3%
Total	5.5%	8.5%

9. Run Plan and Beam Time Request

The running time and experimental conditions described earlier are summarized in table 3 below. The fourth column is the central momentum setting of the HMS, and the fifth column is the invariant mass range that the HMS can cover at that setting. The times are net beam hours. An additional 125 hours for overhead (annealing, Møller and target empty runs and target field rotation) are included.

Experience with the polarized target operation during E143 indicates that data can be taken for periods of 8 to 10 hours with NH_3 and $\sim$ 16 hours with ND_3 before radiation damage reduces the polarization to a level that is too low for efficient data collection. The polarization is restored by annealing the material to about 80 K, in about one hour. Time for 10 anneal cycles is included in the overhead.

The polarization of the beam will be measured at every target change (10-16 hours). About 25 Møller runs (each one hour long) are also included.

Table 3. Run Times and experimental conditions.					
Scattering angle	**B_t Orientation**	**Target**	p_o GeV/c	**Wl- Wh** GeV	**Time** hours
12.5°	Longitudinal	NH_3	4.737	0.938 - 1.710	40
		ND_3			60
		NH_3	4.206	1.470 - 2.000	20
		ND_3			30
Subtotal longitudinal					150
	Transverse	NH_3	4.737	0.938 - 1.710	20
		ND_3			30
		NH_3	4.206	1.470 - 2.000	10
		ND_3			15
Subtotal transverse					75
Subtotal low Q^2 (12.5°)					225
35 °	15° w.r. beam	NH_3	4.589	1.11-1.83	154
Overhead 33%					125
Total					504

The total request is 21 calendar days.

10. Related TJNAF experiments

- Hall C:

There are two approved experiments (93-026 [16] –G_E^n– and 93-028 [17]) that use polarized beam and target in Hall C. The overhead involved in setting up the polarized target is minimized if those experiments and the present proposal are run sequentially (in any convenient order). Experiment 93-028 plans to measure the longitudinal-transverse interference asymmetry A_{LT} in the region of the Δ resonance. That experiment is fundamentally different from the present one, as follows:

- Goal of 93-028 is to extract the scalar quadrupole C_2 at the Δ, ours is to measure all

the spin nucleon asymmetries at low Q^2 and test pQCD and local duality at high Q^2.

- Measured asymmetry is A_{LT}, compared to A_1, A_2, and A_{TT} in the present proposal.

- Target field normal to $\mathbf{q}$, compared to our configuration of fields parallel and perpendicular to the beam for A_1, A_2, and along $\mathbf{q}$ for A_{TT}.

- Target: polarized protons versus both protons and deuterons in our case.

- Mass range from M to $W = 1.4$ GeV, compared to $M \leq W \leq 2$ GeV here.

- Momentum transfer up to 2.5 [GeV/c]^2, versus $\sim$ 5.5 [GeV/c]^2 here, for the relevant quantity A_{TT}.

To correct for the small A_{TT} contributions at the high and low invariant mass ends of the Δ peak, experiment 93-028 will measure this asymmetry at their kinematics for about 10% of their data taking time (7 kinematic settings, 2 to 8 hours per setting, about 30 hours total).

- Hall B:

The spin asymmetries A_1 and A_2 for both protons and deuterons will be studied in experiments 91-023 [26] and 93-009 [27], by measuring the parallel asymmetry at several values of the beam energy and scattering angle. The high Q^2 properties of the resonances with unpolarized beam and targets will be investigated in experiment 91-002. Table 4 below shows details of the relevant quantities involved in each case and in the present proposal.

The goal of our proposal at low Q^2 is to make a precise, high resolution measurement of the invariant mass dependence of the asymmetries, at essentially constant momentum transfer. To this end, we plan to measure both parallel and perpendicular asymmetries, at a single beam energy and scattering angle. The Hall B experiments plans to separate A_1 and A_2 at constant Q^2 by interpolating measurements of $A_{||}$ at several beam energies. The average running time for both NH_3 and ND_3 at each energy is about 400 hours. At least two energies are needed for the separation, or about 800 hours, compared to our 300 hours request.

At our average $Q^2 = 1.3$ [GeV]^2, our resolution for both A_1 and A_2 is 0.2 [GeV]^2 in Q^2 and 30 MeV in W. This is in contrast to the CLAS experiments that take a 30% wider

Q^2 bin for A_1, and a 2.6 times wider one for A_2. The CLAS ΔW resolution for A_1 is like ours (30 MeV), but for A_2 it is twice as wide. These values are listed in the table under the Ranges columns, where in each box the upper numbers represent the range and the lower ones the resolution for each quantity. The CLAS resolutions are adequate for the principal goal of those experiments, which is to study the Q^2 dependence of the DHG sum rule, not the W dependence of A_1 and A_2, as is ours. Both experiments are complementary in that our precise determination of both asymmetries at nearly constant Q^2 must agree with the interpolated CLAS results. Since the spin structure measurements are of the INCLUSIVE scattering type, large solid angle single arm spectrometers such as the HMS are very effective, while the strength of the CLAS lies in EXCLUSIVE multiparticle detection. An obvious advantage of our proposal is the immediate availability of both the polarized target and the Møller polarimeter, facilitating its scheduling.

To illustrate the relative precision of each experiment, we plot in figs. 10 the expected statistical uncertainties, for three conditions:

- a sample of those proposed in Hall B (open triangles),

- the present proposal's (solid circles),

- a sample of the present proposal's normalized to the same resolutions, beam and target polarizations, and dilution factors planned for the CLAS experiments (open crossed circles). Some points are slightly displaced in W for clarity.

The relevant parameters are listed in Table 4. CLAS uses a dilution factor $f = 0.167$ for protons, neglecting the presence of LHe, windows and NMR coils.

Our normalized errors for A_1 are 1.37 times smaller than our expected unnormalized errors, and $\sim$ 4.5 times smaller than Hall B's, on average . Our normalized errors for A_2 are 2.74 times smaller than unnormalized, and $\sim$ 7 times smaller than Hall B's on average. The deuteron errors compare similarly.

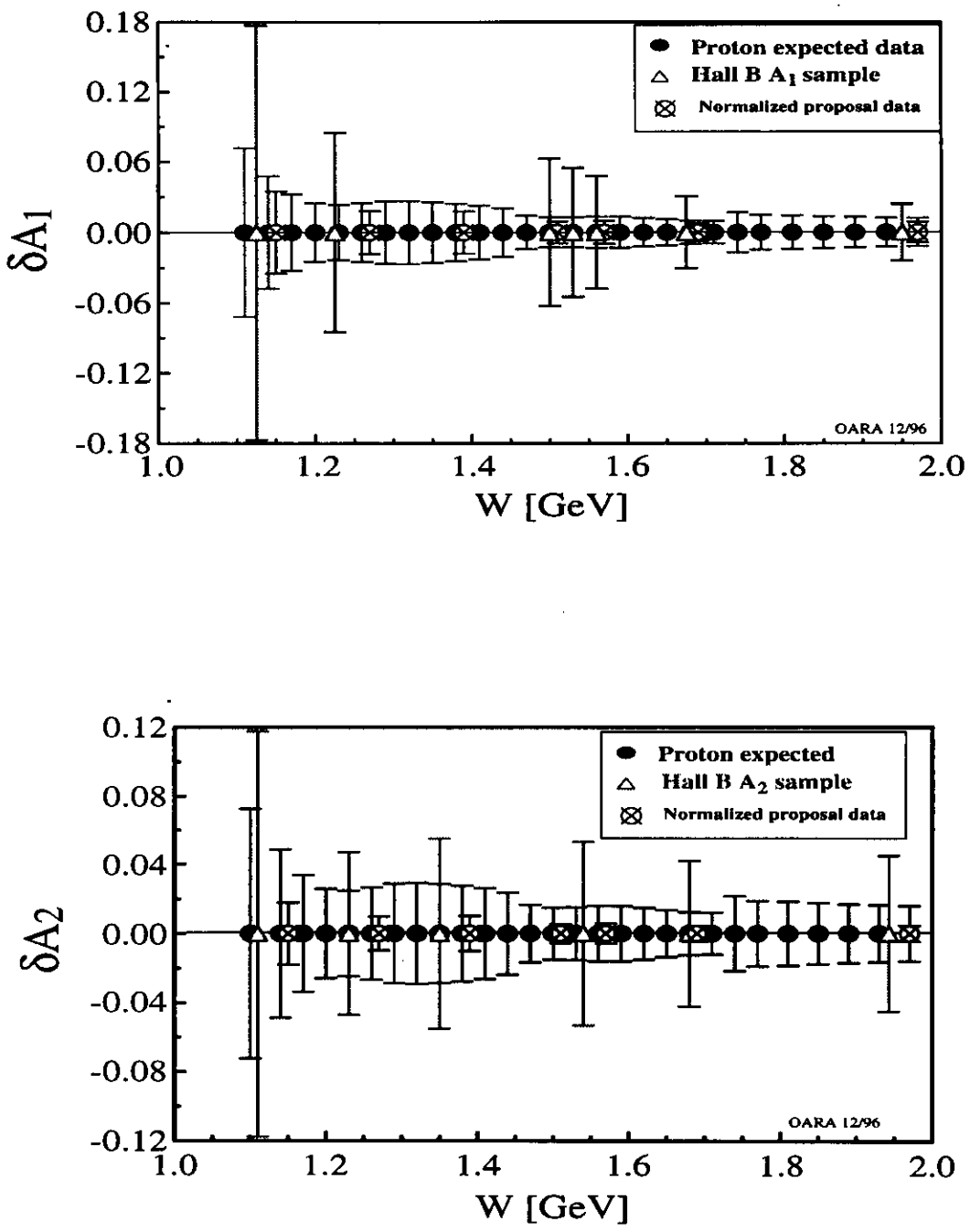

FIG. 10. Comparison of a sample of the proposed statistical errors for the CLAS experiments, with our expected results as proposed and normalized to equal polarizations, resolutions and dilutions. Errors for the proton A_1 (top) and A_2 (bottom) vs W.

At high Q^2 our goal is to test pQCD and polarized local duality, by measuring the asymmetry. Experiment 91-002 plans to measure pion angular distributions, to carry out amplitude decompositions of the resonant transitions. The increasing number of partial waves that already at $Q^2 = 4$ [GeV]^2 have quite substantial influence in the transitions [42], have no bearing on our measurement.

Table 4. Comparative table of Hall B and Hall C experiments.

Proposal No.	Measured Functions	Method	Target (Polariz.)	Beam Energy [GeV] (Polariz.)	Range		Time [h]
					Q^2 (ΔQ^2) [GeV^2]	W (ΔW) [GeV]	
Hall B 91-023	A_1, A_2	$A_\parallel = A_2 + \eta\, A_2$ at several E_{beam}	NH3 (90%)	1.2-6 (80%)	0.2 - 3 (0.2-0.4) xQ2)	1.1 - 2.7 (0.030-0.060)	1000
Hall B 93-009	A_1, A_2	Same as 91-023	ND3 (40%)	4 (75%)	Same as 91-023		960
Hall B 91-002	$A_{1/2}$, $A_{3/2}$	(e, e'π) (e, e' p) π^0,η	H2 unpol.	6 —	>3 - 6 (1.0)	1.2 - 2 (0.050)	768*
Hall C This proposal	A_1, A_2	$A_\parallel$, $A_\perp$	NH3 (85%) ND3 (30%)	6 (80%)	1.3 (0.2)	0.94 - 2. (0.030)	300
	A_{TT}	A_{TT} along $\mathbf{q}$	NH3 (85%)		4.7-5.8 (0.4)	1.1 - 1.83 (0.030)	200

* Concurrent with other Hall B expts.

REFERENCES

[1] E154 collaboration, R. Arnold *et al.* , *Spin Structure Function Using a Polarized HE-3 Target*, SLAC-PROPOSAL-E-154 (1993).

[2] E155 collaboration, R. Arnold *et al.* , *Measurements of Nucleon Spin Structure at SLAC in End Station A*, SLAC-PROPOSAL-E-155 (1993).

[3] SMC collaboration, *Measurements of the Spin-Dependent Structure Functions of the Neutron and the Proton*, Addendum to the NA47 Proposal, CERN/SPSLC 94-13.

[4] M. Dueren and K. Rith *Polarized Electron Nucleon Scattering at HERA: The HERMES Experiment*, in *Hamburg 1991, Proceedings, Physics at HERA, vol. 1* 427-445.

[5] SLAC E130, G. Baum *et al.,* Phys. Rev. Lett. **45**, 2000 (1980).

[6] E143 collaboration, SLAC-PUB-96-7242, September 1996, submitted to Physical Review Letters.

[7] SLAC E80, M. J. Alguard *et al.,* Phys. Rev. Lett. **37**, 1261 (1976); **41**, 70 (1978).

[8] SLAC E130, G. Baum *et al.,* Phys. Rev. Lett. **51**, 1135 (1983).

[9] SLAC E142, P. L. Anthony *et al.,* Phys. Rev. Lett. **71**, 959 (1993).

[10] SLAC E143, K. Abe *et al.*, Phys. Rev. Lett. **74**, 346 (1995).

[11] SLAC E143, K. Abe *et al.*, Phys. Rev. Lett. **75**, 25 (1995).

[12] SLAC E143, K. Abe *et al.*, Phys. Lett. **B364**, 61 (1995).

[13] SLAC E143, K. Abe *et al.*, Phys. Rev. Lett. **76**, 587 (1996).

[14] SMC, D. Adams *et al.*,, Phys. Lett. **B329**, 399 (1994).

[15] SMC, B. Adeva *et al.,* Phys. Lett. **B302**, 533 (1993); SMC, B. Adeva *et al.,* Phys. Lett. **B357**, 248 (1995).

[16] D. Day, spokesman, *The Charge Form Factor of the Neutron*, CEBAF Experiment 93-026.

[17] J. Jourdan, spokesman, *Deformation of the Nucleon*, CEBAF Experiment 93-028.

[18] J. D. Bjorken, Phys. Rev. **148**, 1467 (1966); Phys. Rev. D **1**, 1376 (1970).

[19] S.J. Brodsky, M. Burkardt and I. Schmidt, report No. SLAC-PUB-6087 (1994)

[20] E.D. Bloom and F.J. Gilman, Phys. Rev. Lett. **25**, 1140 (1970); Phys. Rev. D**4**, 2901 (1971).

[21] R. L. Jaffe and Xiangdong Ji, Phys. Rev. **D43**, 726 (1991).

[22] J. L. Cortes, B. Pire and J. P. Ralston, Z. Phys. **C55**, 409 (1992).

[23] SMC, D. Adams, *et al.*, Phys. Lett. **B336**, 125 (1994).

[24] G. G. Petratos *et al.,* Report No. SLAC–PUB–5678 (1991).

[25] V.D. Burkert and B.L. Ioffe, *et al.,* Phys. Lett. **B296**, 223 (1992).

[26] V. Burkert, D. Crabb, R. Minehart, spokespersons, *Measurement of Polarized Structure Functions in Inelastic Electron Proton Scattering using CLAS*, CEBAF Experiment 91-023.

[27] S.E. Kuhn, spokesperson, *The Polarized Structure Function g_1^n and the Q^2 dependence of the Gerasimov-Drell-Hearn Sum Rule for the Neutron*, CEBAF Experiment 93-009.

[28] G. Cates and Z-E. Meziani, spokespersons *Measurement of the Neutron (He) Spin Structure Function at Low Q^2: a Connection between the Bjorken and Drell- Hearn-Gerasimov Sum Rules*, CEBAF experiment 94-010.

[29] C. Carlson, Phys. Rev. D**45**, 2704 (1986).

[30] C. E. Carlson and Wu-Ki Tung, Phys. Rev. D**5**, 721 (1972).

[31] A. J. G. Hey and J. E. Mandula, Phys. Rev. D**5**, 2610 (1972).

[32] P. Stoler, Phys. Rev. Lett. **66**, 1003 (1991); Phys. Rev. D**44**, 73 (1991).

[33] L.M. Stuart, *et al.* , Report No. SLAC–PUB–6316 (1993).

[34] P. Stoler, V. Burkert, M. Taiuti, spokespersons, *The Study of Excited Baryons at High Momentum Transfer with the CLAS Spectrometer*, CEBAF Experiment 91-002.

[35] J. Napolitano*, P. Stoler, spokespersons, *The delta(1232) form Factor at High Momentum Transfer*, CEBAF Experiment 94-014.

[36] F. W. Brasse *et al.* , Nucl. Phys. **B110** (1976) 413.

[37] D. Day, private communication.

[38] L. W. Whitlow *et al.,* Phys. Lett. **B250**, 193 (1990).

[39] L. W. Whitlow *et al.,* Phys. Lett. **B282**, 475 (1992).

[40] T.J. Liu, Doctoral dissertation, Univ. of Virginia, January 1996

[41] A. Abragam, Proc. Int. Symp. on High Energy Phys. with Polarized Beams and Polarized Targets, 1978, Argonne. AIP Conference Proceedings 1979; V. Bouffard *et al.* , J. Physique **12**, 1447 (1980).

[42] Robert W. Lourie, Phys. Rev. C**45**, 450 (1992).